Quantifying the Objective Cost of Uncertainty in Complex Dynamical Systems

Byung-Jun Yoon, *Senior Member, IEEE*, Xiaoning Qian, *Member, IEEE*, and Edward R. Dougherty, *Fellow, IEEE*

***Abstract*—Real-world problems often involve complex systems that cannot be perfectly modeled or identified, and many engineering applications aim to design operators that can perform reliably in the presence of such uncertainty. In this paper, we propose a novel Bayesian framework for objective-based uncertainty quantification (UQ), which quantifies the uncertainty in a given system based on the expected increase of the operational cost that it induces. This measure of uncertainty, called MOCU (mean objective cost of uncertainty), provides a practical way of quantifying the effect of various types of system uncertainties on the operation of interest. Furthermore, the proposed UQ framework provides a general mathematical basis for designing robust operators, and it can be applied to diverse applications, including robust filtering, classification, and control. We demonstrate the utility and effectiveness of the proposed framework by applying it to the problem of robust structural intervention of gene regulatory networks, an important application in translational genomics.**

***Index Terms*—Mean objective cost of uncertainty (MOCU), objective-based uncertainty quantification (UQ), robust network intervention, robust operator design.**

I. Introduction

In many real-world applications, we have to deal with complex systems that cannot be perfectly modeled or accurately identified. The gene regulatory network (GRN) is a perfect example of such a system. The GRN that governs the behavior of living cells consists of tens of thousands of genes that regulate and are regulated by each other. These intertwined dynamical interactions are responsible for the complexities and characteristics of living organisms. Considering the size and the complexity of the GRN, it is obvious that we cannot perfectly describe the network and its dynamics using a mathematical model. For this reason, researchers have been using simplified models, such as the Boolean network (BN) or the probabilistic Boolean network (PBN), to model and study GRNs [1]. However, even for these simple models, the model complexity quickly grows with increasing number of genes, which makes it very difficult to accurately estimate these models from observed data. Similarly, in many real-world problems, the system of interest may not be accurately identified due to its inherent complexity, insufficient training data, or both.

Despite the difficulty of accurate system identification, various engineering problems aim at performing optimal operations—be it filtering, classification, or control—based on a system of interest, in the presence of substantial uncertainty. A well-known example is robust filtering. Qualitatively, a filter is said to be *robust* when its performance degradation is acceptable for signals that are statistically close to those for which it has been designed. The problem of robustness arises because optimizing the filter is relative to a signal model, which in this case is uncertain. For example, the work of Kuznetsov on signal detection [2] and Kassam on Wiener filtering [3] are concerned about cases when the relevant spectra are not perfectly known, which is also addressed by the theory of minimax robustness by Poor and colleagues [4]–[6]. More recent examples include the work on Bayesian robustness in the design of morphological filters [7], classification [8], and control of GRNs [9].

An important relevant question that arises when dealing with systems (or models) with uncertain characteristics is the following: how can we quantify the uncertainty that is present in a given system (or model) in a meaningful and practically useful manner? Traditionally, such uncertainty has been often measured in terms of entropy. For example, several studies on GRN inference have considered the problem of designing optimal gene perturbation experiments that can maximally reduce the entropy of the potential network models [10], [11]. In this paper, we propose an effective Bayesian framework that aims to address the previous question from a different angle. In the proposed framework, the uncertainty of a given system is quantified in an objective-oriented manner based on the expected increase of the operational cost that it induces, rather than the entropy. The proposed uncertainty measure, referred to as MOCU (mean objective cost of uncertainty), provides a practical way of quantifying the effect of the present uncertainty on the operation of interest. The proposed objective-based UQ (uncertainty quantification) framework provides a general mathematical basis for designing robust operators, and it can be applied to various applications, including robust filtering, classification, and control.

The organization of this paper is as follows. Section II lays out the theoretical framework of objective-based UQ and presents an illustrative example based on hidden state prediction in an uncertain hidden Markov model (HMM) to show the importance of objective-based UQ. In Section III,

Manuscript received April 16, 2012; revised December 18, 2012; accepted February 17, 2013. Date of publication March 07, 2013; date of current version April 09, 2013. The associate editor coordinating the review of this manuscript and approving it for publication was Dr. Yufei Huang. The work of B.-J. Yoon was supported in part by the National Science Foundation through NSF Award CCF-1149544. The work of X. Qian was supported in part by the National Institute of Diabetes and Digestive and Kidney Diseases, National Institutes of Health —Award R21DK092845.

B.-J. Yoon is with the Department of Electrical and Computer Engineering, Texas A&M University, College Station, TX 77843 USA (e-mail: bjyoon@ece.tamu.edu).

X. Qian is with the Department of Computer Science and Engineering, University of South Florida, Tampa, FL 33620 USA.

E. R. Dougherty is with the Department of Electrical and Computer Engineering, Texas A&M University, College Station, TX 77843 USA. He is also with the Translational Genomics Institute (TGen), Phoenix, AZ 85004 USA.

Color versions of one or more of the figures in this paper are available online at http://ieeexplore.ieee.org.

Digital Object Identifier 10.1109/TSP.2013.2251336

we discuss the derivation of robust operators based on the proposed framework. In Section IV, we focus on the application of objective-based UQ and robust operator design to an important problem in genomic signal processing (GSP): namely, the derivation of robust structural intervention strategies in regulatory networks to reduce the risk of entering aberrant phenotypes. Finally, we conclude the paper in Section V.

II. Objective-Based Uncertainty Quantification (UQ)

A. Mean Objective Cost of Uncertainty (MOCU)

Suppose we want to design a robust operator with respect to a model that is uncertain. In the context of robust operator design, we are not as much concerned about the uncertainty of the system itself as the performance of the operator that needs to be designed in the presence of this uncertainty. For example, consider the case when our goal is to find the optimal filter with respect to a signal model, where some of the parameters are not known with certainty and can vary substantially. However, as long as these parameters do not affect the overall performance of the designed filter, the model uncertainty will not be a concern at all. On the other hand, when there exist parameters that may significantly degrade the filter performance in case of small mismatch, the model uncertainty would indeed matter. From a practical perspective, this implies that: (i) the uncertainty of a given model should be understood based on the *objective* of employing the model (e.g., signal estimation) and (ii) this uncertainty has to be quantified in terms of the expected *cost* it induces (e.g., estimation error), with respect to an operator class.

To formulate this idea in a formal manner, let us consider a model defined by a parameter vector θ from a class Θ of parameter vectors—or equivalently, a class of models—governed by a prior distribution $f(\theta)$. This distribution may come from observation data and/or prior knowledge regarding the model. We assume that there exist a family Ψ of operators and a family $\Xi = \{\xi_\theta | \theta \in \Theta\}$ of cost functions $\xi_\theta : \Psi \to [0, \infty)$. In the presence of uncertainty in θ, our goal is to design a robust operator,

$$\psi^* = \arg\min_{\psi \in \Psi} E_\theta \left[\xi_\theta(\psi)\right], \tag{1}$$

which minimizes the expected cost. Although it is possible to measure the uncertainty in terms of the entropy of the model θ based on its distribution $f(\theta)$—with the entropy being 0 when there is no uncertainty—the entropy does *not* tell us much about the operator performance. The entropy could be large, but if the networks in Θ are very close to each other with regard to whatever network characteristics determine the operators, the fact that the entropy is large is of little consequence. In the other direction, the entropy could be small, but the networks be far apart with regard to the characteristics determining the operators, which would be of significant consequence. With this in mind, for a specific model with parameter vector θ, we define the *objective cost of uncertainty (OCU)* relative to $\theta \in \Theta$ as the differential cost of using the robust operator ψ^* instead of the operator ψ_θ that is optimal for the given model:

$$U_{\Psi,\Xi,f}(\Theta, \theta) = \xi_\theta(\psi^*) - \xi_\theta(\psi_\theta). \tag{2}$$

The overall cost of uncertainty can be computed by taking its expectation over $f(\theta)$,

$$\mathrm{M}_{\Psi,\Xi,f}(\Theta) = E_\theta \left[U_{\Psi,\Xi,f}(\Theta, \theta)\right], \tag{3}$$

which we call the *mean objective cost of uncertainty (MOCU)*. The objective cost of uncertainty is relative to the operator family Ψ and the family Ξ of cost functions, in addition to the uncertainty distribution $f(\theta)$, thereby taking into account the *objective* of operator design, be it signal estimation, classification, or control.

The proposed UQ framework and the concept of MOCU has important connections to existing techniques and concepts that have been used in various fields. For example, the robust operator ψ^* can be viewed as a Bayesian estimator [12] that minimizes the expected cost over all potential models $\theta \in \Theta$. Similarly, we can view the MOCU as the minimum expected value of a Bayesian loss function, where the Bayesian loss function maps an operator to its differential cost (for using the given operator instead of the optimal operator) and its minimum expectation is attained by the optimal robust operator that minimizes the average differential cost. This differential cost has been often referred to as the *regret* in decision theory [13], which is defined as the difference between the maximum payoff (for making the optimal decision) and the actual payoff (for the decision that has been made). From this perspective, the MOCU can also be viewed as the minimum expected regret for using the robust operator.

Traditionally, model uncertainty has been extensively studied under the Bayesian framework [14]–[16]. The Bayesian approach provides a general framework for handling model uncertainty, where the uncertainty can be represented by a prior distribution of the model and subsequently updated upon the arrival of new data to obtain a posterior distribution. Under this framework, two major research thrusts in model uncertainty have been *model selection* [17]–[19] and *model averaging* [20]–[22], where the former concerns choosing the most probable model in the presence of uncertainty, whereas the latter concerns finding the "average model" by incorporating uncertainty. There has been a significant amount of research on both problems [15], [23], which has been accompanied and accelerated by advances in computational methods for posterior computation [24].

Despite these mathematical and conceptual ties, it should be noted that the above concepts and approaches have not been widely used for "uncertainty quantification" *per se*. For example, research on model uncertainty under the classical Bayesian framework has mainly focused on model identification in the presence of uncertainty, be it through model selection or model averaging, rather than quantifying the uncertainty present in the model. In fact, model uncertainty has been traditionally measured using entropy [10], [11], without giving due consideration to the practical objective of employing (or inferring) the model.

B. An Illustrative Example: Hidden Markov Model with Uncertain Parameters

The MOCU defined in (3) can provide an effective means of quantifying model uncertainty in diverse applications. As an

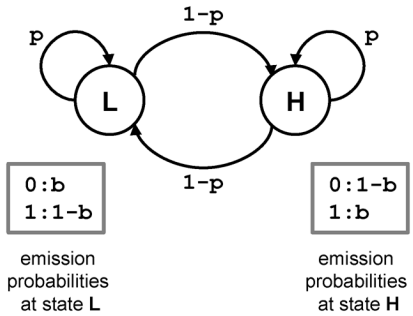

Fig. 1. Hidden Markov model with two states $\mathbf{L}$ and $\mathbf{H}$. The parameter p determines the transition probabilities between states and b determines the symbol emission probabilities at the respective states.

illustrative example, let us consider a simple hidden Markov model (HMM) shown in Fig. 1. The HMM has two hidden states $\mathbf{L}$ and $\mathbf{H}$, and the model generates a sequence $\mathbf{x} = x_1 x_2 \cdots x_L$ of binary symbols $x_k \in \{0, 1\}$. As shown in Fig. 1, the emission probabilities of the HMM are determined by the parameter $b \in [0, 1]$, and the transition probabilities are governed by the parameter $p \in [0, 1]$. Given a symbol sequence $\mathbf{x}$, suppose we want to predict the state y_L in the underlying hidden state sequence $\mathbf{y} = y_1 y_2 \cdots y_L$. If the parameter vector $\theta = (b, p)$ is known, we can make optimal predictions using the following operator $\psi_\theta(\mathbf{x})$

$$\hat{y}_L = \psi_\theta(\mathbf{x}) = \begin{cases} 0, & \text{if } P(y_L = 0|\mathbf{x}) \geq P(y_L = 1|\mathbf{x}) \\ 1, & \text{if } P(y_L = 0|\mathbf{x}) < P(y_L = 1|\mathbf{x}) \end{cases}.$$

This operator minimizes the expected prediction error

$$\begin{aligned} \xi_\theta(\psi_\theta) &= E_{\mathbf{x}} \left[I\{\hat{y}_L \neq y_L\} \right] \\ &= \sum_{\mathbf{x}} P(\mathbf{x}) \min \left\{ P(y_L = 0|\mathbf{x}), P(y_L = 1|\mathbf{x}) \right\}. \end{aligned}$$

Given a HMM, the probabilities $P(\mathbf{x})$ and $P(y_L|\mathbf{x})$ can be efficiently computed using the forward algorithm [25].

Now, let us consider the case when the model is not perfectly known. What would be the cost (i.e., prediction error) for using an operator obtained based on an inaccurate estimate $\hat{\theta}$ instead of the true θ? Fig. 2 shows the prediction error when there is mismatch between the true b and its estimate $\hat{b}$, where the length of the observed symbol sequence $\mathbf{x}$ is set to $L = 5$. Let us first consider the case when $p = 0.75$. As we can see from Fig. 2(a) (and the corresponding contour plot in Fig. 2(c)), a mismatch between b and $\hat{b}$ does not affect the prediction error at all, as long as both of them belong to [0,0.5) or (0.5,1]. For example, when $b = 0.1$, any operator obtained based on an inaccurate estimate $\hat{b} \in [0, 0.5)$ will yield the same error (which is 0.1) as the optimal operator that uses the true parameter. On the other hand, any other operator obtained using $\hat{b} \in (0.5, 1]$ will give a much larger error (which is 0.9). The results are similar for $p = 0.99$, as shown in Fig. 2(b) and Fig. 2(d). Suppose we have two different uncertainty classes of HMMs, where the first class contains models with a parameter vector $\theta \in \Theta_1 = \{(b, p)|b \in [0.1, 0.4], p = 0.75\}$ and the second class contains models with $\theta \in \Theta_2 = \{(b, p)|b \in [0.45, 0.55], p = 0.75\}$, where θ is assumed to be uniformly distributed in each of these classes.

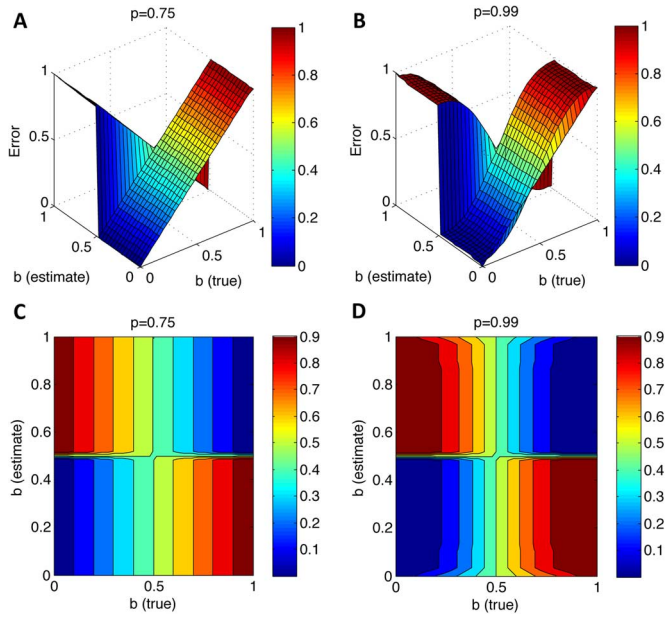

Fig. 2. Cost of mismatch in the parameter b. (A,C) Decoding error and its contour plot when $p = 0.75$. (B,D) Decoding error and its contour plot when $p = 0.99$.

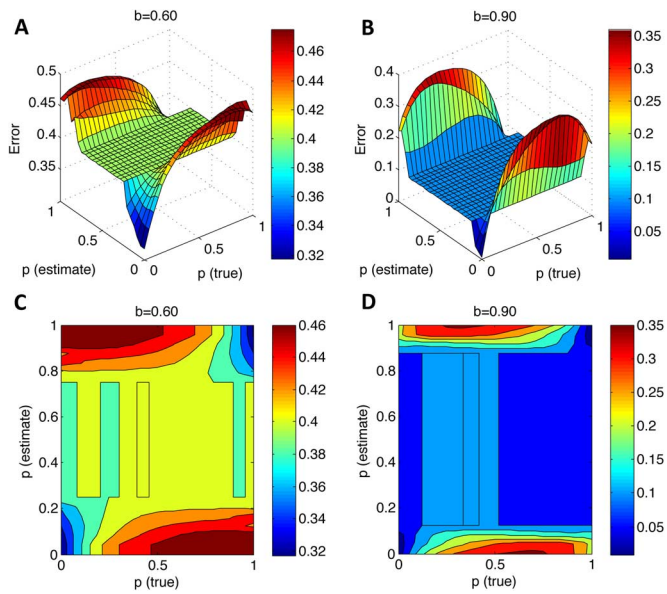

Fig. 3. Cost of mismatch in the parameter p. (A,C) Decoding error and its contour plot when $b = 0.60$. (B,D) Decoding error and its contour plot when $b = 0.90$.

Which among the two classes has larger uncertainty? A simple approach based on the variation of the model parameters would choose Θ_1 over Θ_2, but Fig. 2 clearly shows that it is the other way around.

Fig. 3. shows the prediction error when p is not accurately known. Let us assume $b = 0.6$ and consider two uncertainty classes $\Theta_3 = \{(b, p)|p \in [0.3, 0.7], b = 0.6\}$ and $\Theta_4 = \{(b, p)|p \in [0, 0.1], b = 0.6\}$. As before, we assume a uniform distribution for both classes. As we can see from Fig. 3(a) and Fig. 3(c), there will not be any cost of uncertainty for the class Θ_3, since any operator based on a (possibly inaccurate) estimate

TABLE I
THE MEAN OBJECTIVE COST OF UNCERTAINTY (MOCU) OF THE HMM IN FIG. 1 WHEN THE PARAMETER b IS NOT PERFECTLY KNOWN

parameter uncertainty	optimal	robust	MOCU
$p = 0.75,\ 0.00 \le b \le 0.04$	0.002	0.002	0.000
$p = 0.75,\ 0.04 \le b \le 0.08$	0.006	0.006	0.000
$p = 0.99,\ 0.00 \le b \le 0.04$	9.70e-3	1.10e-2	1.27e-3
$p = 0.99,\ 0.04 \le b \le 0.08$	1.63e-2	1.63e-2	0.000
$p = 0.99,\ 0.47 \le b \le 0.51$	0.477	0.482	4.54e-3

TABLE II
THE MEAN OBJECTIVE COST OF UNCERTAINTY (MOCU) OF THE HMM IN FIG. 1 WHEN THE PARAMETER p IS NOT PERFECTLY KNOWN

parameter uncertainty	optimal	robust	MOCU
$b = 0.60,\ 0.00 \le p \le 0.20$	0.368	0.371	3.35e-3
$b = 0.60,\ 0.20 \le p \le 0.40$	0.399	0.400	2.46e-4
$b = 0.60,\ 0.35 \le p \le 0.55$	0.400	0.400	0.000
$b = 0.90,\ 0.00 \le p \le 0.20$	8.28e-2	0.100	1.72e-2
$b = 0.90,\ 0.20 \le p \le 0.40$	0.100	0.100	0.000
$b = 0.90,\ 0.35 \le p \le 0.55$	0.100	0.100	0.000

$\hat{p} \in [0.3, 0.7]$ will perform as well as the optimal operator constructed from the true $p \in [0.3, 0.7]$. On the other hand, the cost of uncertainty will be significant for the class Θ_4, since there will be a substantial performance difference between the optimal operator, based on the true p, and a suboptimal operator, obtained from an inaccurate estimate $\hat{p} \neq p$, despite the narrower range of p. Similar observations can be made in Fig. 3(b) and Fig. 3(d), when $b = 0.9$.

These examples clearly show that the uncertainty in a given model cannot be effectively quantified simply based on the variation (or entropy) of the parameters that define the model. Instead, UQ should be driven by the ultimate objective for employing the model, in the context of an operator class. From this perspective, the concept of MOCU proposed in this section can provide a general and effective framework for quantifying the uncertainty of various models, in case they are only partially known and cannot be accurately estimated. For example, suppose we are interested in designing biological experiments to improve the inference of a complex gene regulatory network as in [10], [11]. From a practical perspective, considering that perfect identification of the network is impossible, it would be more beneficial to design the experiments that can maximally reduce the MOCU rather than the entropy of the network uncertainty class, since the reduction of the MOCU will have a direct impact on the performance of the robust operator to be constructed based on the reduced uncertainty class.

Based on (3), we computed the MOCU of the HMM shown in Fig. 1 (with $L = 5$), for several cases when the parameter vector $\theta = (b, p)$ is only partially known and is uniformly distributed in the corresponding uncertainty class Θ. First, we considered the case when the parameter p is perfectly known while we only know the range of b. Table I shows the estimated MOCU for this case. The first column in the table shows the value of p and the range of b. The second column shows the mean cost (i.e., the mean prediction error) $E_\theta[\xi_\theta(\psi_\theta)]$ of the optimal operator that has perfect knowledge of θ. The third column shows the mean cost $E_\theta[\xi_\theta(\psi^*)]$ of the optimal robust operator ψ^*, which can be obtained from (1). Finally, the fourth column shows the MOCU, which is defined as the expected differential cost for using the robust operator, instead of the optimal operator, for each model in the uncertainty class of HMMs that arises from an imperfect knowledge of b. As can be seen in Table I, without a formal UQ framework, it is practically impossible to compare the relative amount of uncertainty across different cases. We can draw a similar conclusion based on the results in Table II, which shows the MOCU for the case when b is perfectly known, while only the range is known for p.

III. DESIGNING ROBUST OPERATORS IN THE PRESENCE OF UNCERTAINTY

The proposed UQ framework provides a natural basis for designing robust operators that are optimal in terms of average performance. In the past, there has been significant research on designing robust filters based on the *minimax* approach, which aims to build a filter whose worst performance over an uncertainty class of models Θ is best among all filters. Minimax robust linear filters have been studied in terms of both the signal-to-noise ratio and signal-noise power spectra pairs [2]–[5], [26]. Minimax robustness has been also applied in other linear optimization frameworks, including matched filtering and Kalman filtering, [6], [27]–[30], and a general formulation has been developed in the context of game theory [6]. The downside of minimax robust filtering is that, in avoiding the worst-case scenario, the average performance of the designed filter can be poor.

The Bayesian approach adopted in this paper can effectively address this issue. In fact, the robust operator ψ^* in (1) is optimal in terms of average performance across all models in the uncertainty class Θ, minimizing the expected cost of the uncertainty that is present in the model. We call this an *intrinsically Bayesian robust (IBR)* operator, and denote it as $\psi_{\mathrm{IBR}} \triangleq \psi^*$, because its optimality is across the full operator family. This IBR operator provides wider optimality with respect to robustness than the previously proposed Bayesian robust approach [7]–[9], which involves designing an optimal operator $\psi_{\hat{\varphi}}$ specific to a model $\hat{\varphi}$ according to

$$\psi_{\hat{\varphi}} = \arg \min_{\psi_\varphi : \varphi \in \Theta} E_\theta \left[\xi_\theta(\psi_\varphi) \right], \tag{4}$$

where $\hat{\varphi} = \arg\min_{\varphi \in \Theta} E_\theta[\xi_\theta(\psi_\varphi)]$ is called the *maximally robust state*. We refer to the resulting operator $\psi_{\hat{\varphi}}$ as a *model-constrained Bayesian robust (MCBR)* operator and denote it as $\psi_{\mathrm{MCBR}} \triangleq \psi_{\hat{\varphi}}$. Note that the optimality of a MCBR operator is only across the set of model-specific optimal operators, as opposed to the IBR operator defined in (1), where the optimization has no such restriction.

While the original Bayesian robust operator theory did not employ the notion of MOCU, if we restrict optimization to network-specific optimal operators, hence use the MCBR operator ψ_{MCBR} instead of the IBR operator ψ_{IBR} for computing the objective cost of uncertainty, we get the following *model-constrained OCU* relative to θ:

$$U^{\mathrm{mc}}_{\Psi,\Xi,f}(\Theta, \theta) = \xi_\theta(\psi_{\mathrm{MCBR}}) - \xi_\theta(\psi_\theta). \tag{5}$$

Taking the expectation over $f(\theta)$ yields model-constrained MOCU, namely,

$$\mathrm{M}^{\mathrm{mc}}_{\Psi,\Xi,f}(\Theta) = E_\theta\left[U^{\mathrm{mc}}_{\Psi,\Xi,f}(\Theta,\theta))\right], \tag{6}$$

which gives us an upper bound on the true MOCU, such that

$$\mathrm{M}_{\Psi,\Xi,f}(\Theta) \le \mathrm{M}^{\mathrm{mc}}_{\Psi,\Xi,f}(\Theta). \tag{7}$$

Clearly the IBR operator is preferable to the MCBR operator, since the minimum is taken over a larger class of operators. Moreover, we would certainly prefer to know the MOCU rather than an upper bound on it. There are, however, two reasons why MCBR operators might be useful. First, it may be practically easier to find a MCBR operator. For instance, in the case of stationary network control, MCBR operators can be found using dynamic programming for each $\theta \in \Theta$ as shown in [9], whereas IBR operators cannot be found in such a way. In the case of finite-state discrete-time networks, there is a finite number of stationary controllers, but the number of them is huge once the network is beyond several genes. In general, whereas one may be able to find an IBR operator by exhaustive search, this may be computationally infeasible. Thus, we may have to be content with MCBR operators and the model-constrained MOCU as an approximation to the true MOCU. A second advantage of MCBR operators is the ability to obtain closed-form analytic solutions in some situations.

To illustrate the latter advantage of MCBR operators, let us consider a classical signal processing example: recovery of a signal Y via a linear filter from a blurred signal plus additive noise,

$$X_\theta(t) = \int_{-\infty}^{\infty} h_\theta(\tau)Y(t-\tau)\mathrm{d}\tau + N(t), \tag{8}$$

where $h_\theta(\tau)$ is a blurring function, depending on the state θ of the system, with Fourier transform $H_\theta(\omega)$. We assume $X(t)$ is wide-sense stationary with autocorrelation function $r_X(\tau)$ and power spectral density $S_X(\omega)$. Given the state θ, the Wiener filter,

$$\psi_\theta(\omega) = \frac{\bar{H}_\theta(\omega)S_Y\omega)}{|H_\theta(\omega)|^2 S_Y(\omega) + S_N(\omega)}, \tag{9}$$

is optimal relative to mean-square error (MSE), but we do not know the state. Let $\xi_\theta(\psi_\varphi)$ denote the MSE for applying the optimal filter for state φ to the degraded signal in system θ. The expected increase of error from using ψ_φ instead of the optimal filter for the actual system state, $E_\theta[\xi_\theta(\psi_\varphi) - \xi_\theta(\psi_\theta)]$, is known as the *mean robustness* of the filter ψ_φ. Minimizing $E_\theta[\xi_\theta(\psi_\varphi)]$ is the same as minimizing $E_\theta[\xi_\theta(\psi_\varphi) - \xi_\theta(\psi_\theta)]$, so that minimizing the mean robustness gives a maximally robust state. Assuming the noise is white, for the convolution model of (8), one can express $\xi_\theta(\psi_\varphi) - \xi_\theta(\psi_\theta)$ in closed form [31]. Because the expression is quite complicated and our purpose here is for illustration, we provide only the special case where there is no additive noise, in which case one obtains

$$\xi_\theta(\psi_\varphi) - \xi_\theta(\psi_\theta) = \frac{1}{2\pi}\int_{-\infty}^{\infty} \frac{|H_\theta(\omega) - H_\varphi(\omega)|^2 S_Y(\omega)}{|H_\varphi(\omega)|^2}\mathrm{d}\omega. \tag{10}$$

Taking the expectation with respect to θ gives the mean robustness for state φ. Minimizing the mean robustness over φ yields the MCBR filter and the model-constrained MOCU. The derivation of (10) requires a MCBR (state-specific or model-constrained) approach. Although the MOCU is unknown for the signal-plus-noise model, we have an upper bound in terms of the Fourier transform of the blurring function and the prior distribution on the uncertainty class, in the form of the expectation over this distribution. We can see from (10) that, if $E_\theta[|H_\theta(\omega) - H_{\hat{\varphi}}(\omega)|^2]$ is small, where $\hat{\varphi}$ is a maximally robust state, then the model-constrained MOCU is small, so that the true MOCU itself must be small. Moreover, our uncertainty of the blurring function mainly matters where the mass of $S_Y(\omega)$ is concentrated, because regions for which $S_Y(\omega) \approx 0$ contribute very little to the integral in (10).

IV. Application: Robust Structural Intervention in Boolean Networks in the Presence of Uncertainty

In this section, we consider the problem of robust structural intervention in gene regulatory networks to demonstrate the utility and effectiveness of the proposed objective-based uncertainty quantification framework. Specifically, we focus on the robust structural intervention in the probabilistic Boolean network (PBN) model [1], [32] in the presence of model uncertainty. A PBN is a stochastic extension of the classical Boolean network (BN) [33], which has been shown to be effective in modeling nonlinear relationships among molecules and capturing the switching behavior in many biological processes, including the cell cycle [34]–[37]. In recent years, PBNs have been actively studied to understand the stochastic behavior of genetic regulatory networks, and especially, to design systematic network-based intervention strategies to achieve beneficial dynamic changes [1], [38].

A. Review of Probabilistic Boolean Network (PBN) and Network Intervention

In the binary version of a PBN with n molecules, the expression state x_i for molecule i can either be "ON" or "OFF", denoted by 1 and 0, respectively. In general, PBNs do not require binary expression states, but here we restrict ourselves to binary values because these apply to our application at hand. At time $t+1$, the expression state $x_i \in \{0,1\}$ is determined by a predictor Boolean function chosen from a set, $\mathbf{f}_i = \{f_i^1, f_i^2, \ldots, f_i^{C_i}\}$, of predictor functions, where the input of a predictor function $f_i^c : \{0,1\}^{K_i} \mapsto \{0,1\}$ consists of the expression states of its K_i regulators in the network at time t. At any time t, the network transition is defined by n predictor functions, one from each $\mathbf{f}_i \in \mathbf{F} = \{\mathbf{f}_1, \mathbf{f}_2, \ldots, \mathbf{f}_n\}$ for each gene $i = 1, \cdots, n$. Each such set of n predictor functions determines a constituent network, or *context*, of the PBN, which is characterized by a collection of m contexts. At each time point, there is a positive probability q of switching contexts and, if a decision is made to switch, there is a selection probability distribution, $\{s_1, s_2, \ldots, s_m\}$, governing the random selection of a context. Switching can occur in two ways. In an *instantaneously random* PBN, we have $q = 1$, so that a context selection occurs at every time point; in a context-sensitive PBN,

we have $q < 1$, so that a context (set of transition rules) remains in place until a decision for a switch occurs. Another source of stochasticity arises in the form of a perturbation probability p, governing random perturbations of expression states. There are several different transition rules, which include the "majority vote" rule [37], [39] and the "strong inhibition" rule [40]. State transitions can either be synchronous or asynchronous [35], [40], [41]. If $C_i = 1$ for all i, then the model becomes a Boolean network with perturbation (BNp). Further, when we set $p = 0$, the model becomes a classical deterministic BN. In this paper, we will focus on the robust structural intervention of BNps.

The underlying network dynamics of PBNs can be modeled as a finite Markov chain. Given the probabilistic parameters of a PBN, we can derive the state transition diagram of the corresponding Markov chain and analyze the network dynamics via the classical Markov chain theory [42], [43]. The underlying Markov chain of a PBN is irreducible and ergodic when $p > 0$. Hence, the network possesses a steady-state distribution (SSD) π such that $\pi^T = \pi^T P$, where P is the transition matrix determined by the network model, and T denotes transpose. The SSD reflects the long-term behavior of a PBN, and the change of SSD by different types of perturbations may guide the design of beneficial intervention strategies [38], [44], [45].

Recent studies on the design of network intervention strategies in PBNs have mainly focused on two basic categories of intervention approaches: *external control* [46] and *structural intervention* [38]. External control involves stationary control policies to flip (or not flip) the expression state of a control gene to steer the system away from "undesirable" dynamics corresponding to aberrant cellular phenotypes to "desirable" network behavior. This type of network intervention corresponds to intervention using drugs to act on gene products. In this paper, we will focus on the second type of network intervention, structural intervention, which aims to optimally change the wiring of gene regulatory relationships so that the determining regulatory functions and, hereafter, the state transitions of the underlying Markov chain are altered for beneficial dynamic changes. In molecular biology, there exist advanced techniques to carry out such interventions for "pathway blockage". To be specific, we study structural perturbation to model the siRNA interference of regulatory relationships, in which we assume that we can block the regulation between any two genes in the network using siRNAs. Mathematically, the perturbed network will have a perturbed transition matrix $\tilde{P}$ with a new SSD $\tilde{\pi}$. Typically, the network state space is partitioned into two sets U and D of *undesirable* and *desirable states* reflecting abnormal and healthy phenotypes, often according to the expression states of a given set of genes. We aim to find the optimal structural intervention that minimizes the probability mass $\tilde{\pi}_U = \sum_{\mathbf{x}\in U} \tilde{\pi}_{\mathbf{x}}$, where $\tilde{\pi}_{\mathbf{x}}$ denotes the perturbed steady-state probability at a given network expression state $\mathbf{x}$.

B. Model Uncertainty, MOCU, and Robust Structural Intervention

To design robust structural intervention strategies, we first define the uncertainty of PBNs based on the concept of MOCU proposed in this paper. As defined in (3) in Section II, we consider the average difference in the effectiveness of (i) designing a model-specific structural intervention based on full knowledge of the network and that of (ii) designing a robust policy that takes into account the uncertainty in the network model.

Model uncertainty is commonplace in dynamical models for biological networks, as we still lack accurate and complete information regarding the regulatory relationships among genes [47]. Currently, existing studies of network robustness and controllability [37], [48]–[51] mostly focus on network topology alone (i.e., presence or absence of molecular binding), ignoring the actual regulatory relationships between genes (i.e., activation or suppression of a given gene by another gene), and therefore may not capture the critical network dynamic properties. We consider a class Θ of PBNs, in which we have *partial* knowledge of regulatory relationships. We assume that Θ is a class of PBNs that arise due to the lack of knowledge of the actual activating or suppressing regulatory relationships between pairs of nodes that govern network transitions. Hence, the parameter vector θ relative to the uncertainty class Θ describes the activating or suppressing relationships for certain edges in the PBNs. We define

$$R_{j\to i} = \begin{cases} 1 & j \text{ activates } i \\ 0 & j \text{ does not regulate } i \\ -1 & j \text{ suppresses } i \end{cases}$$

as the regulatory relationship between gene i and j. We assume that there are D pairs of genes (j, i) in the network, for which the *existence* of a regulatory relationship is known based on the available prior knowledge but the *type* of the relationship (activating or suppressing) is not exactly known. As a result, the network uncertainty class Θ will consist of 2^D possible networks, where each network $\theta \in \Theta$ corresponds to a specific assignment of regulation types to the D uncertain edges. We further assume that the uncertainty class Θ is governed by a uniform prior distribution $f(\theta)$ over all $\theta \in \Theta$. Our analysis extends to other distributions in a straightforward manner.

For robust structural intervention, we define a family Ψ of structural intervention operators that block the regulatory action between regulatory pairs of genes in the network by setting $R_{j'\to i'} = 0$. These operators model pathway blockage through siRNA interference. We allow an operator to block only one regulation: $\psi \in \Psi$ selects an existing regulation and blocks it. Since our ultimate goal is to minimize the steady-state mass of undesirable states to achieve beneficial dynamic changes in the network, our objective function is the total undesirable steady-state mass, $\tilde{\pi}^{\theta}_U(\psi) = \sum_{\mathbf{x}\in U} \tilde{\pi}^{\theta}_{\mathbf{x}}(\psi)$, where $\tilde{\pi}^{\theta}_{\mathbf{x}}(\psi)$ denotes the steady-state probability of the network state $\mathbf{x}$ after applying structural intervention ψ to a given network θ in the uncertainty class Θ. Hence, the family Ξ is a set of cost functions $\xi_\theta(\psi) = \tilde{\pi}^{\theta}_U(\psi) : \Psi \to [0, 1]$. To derive IBR structural intervention, we aim to minimize the expected total undesirable steady-state mass by structural intervention with respect to the uncertainty class Θ:

$$\psi^* = \arg\min_{\psi\in\Psi} \mathbf{E}_\theta \left[\tilde{\pi}^{\theta}_U(\psi)\right]. \tag{11}$$

For a specific PBN with given regulatory relationships θ, its objective cost of uncertainty measures the differential cost of using the robust operator ψ^* instead of the optimal network-

specific operator ψ_θ: $U_{\Psi,\Xi,f}(\Theta,\theta) = \tilde{\pi}^\theta_U(\psi^*) - \tilde{\pi}^\theta_U(\psi_\theta)$. By taking its expectation over $f(\theta)$, which we assume to be uniform, we can obtain the MOCU for structural intervention in PBNs, as defined in (3). Similarly, we may derive the MCBR structural intervention $\psi_{\hat{\varphi}} = \arg\min_{\psi_\varphi:\varphi\in\Theta} \mathbf{E}_\theta[\tilde{\pi}^\theta_U(\psi_\varphi)]$, in which $\hat{\varphi} = \arg\min_{\varphi\in\Theta} \mathbf{E}_\theta[\tilde{\pi}^\theta_U(\psi_\varphi)]$ is the maximally robust state. By comparing the effectiveness of this MCBR intervention strategy with that of model-specific optimal structural intervention (with full knowledge of θ), we can derive the *model-constrained OCU* relative to θ as: $U^{\mathrm{mc}}_{\Psi,\Xi,f}(\Theta,\theta) = \tilde{\pi}^\theta_U(\psi_{\hat{\varphi}}) - \tilde{\pi}^\theta_U(\psi_\theta)$. By taking its expectation over $f(\theta)$, we can obtain the model-constrained MOCU (6) for structural intervention in PBNs.

C. Robust Structural Intervention in the Yeast Cell Cycle Network

In this section, we assess the performance of the IBR structural intervention ψ^*, as defined in (1), and compare it with that of the MCBR structural intervention $\psi_{\hat{\varphi}}$, which is designed based on a specific network $\hat{\varphi} \in \Theta$ that minimizes the cost as defined in (4). More specifically, we generate random ensembles of BNps, where each ensemble constitutes an uncertainty class of networks, and investigate the chances that the IBR and MCBR operators will lead to different expected costs for a given uncertainty class.

We take two different approaches to create the random ensembles of BNps. In the first approach, random networks are generated by a specific class of regulatory functions using the "majority vote" rules, which have been used in the literature for modeling the budding yeast (*Saccharomyces cerevisiae*) cell cycle network [35], [37], [39]. The dynamics of x_i are determined by the following majority voting rules:

$$f_i(\mathbf{x}) = \begin{cases} 1 & \text{if } \sum_j R_{j\to i}x_j > 0 \\ x_i & \text{if } \sum_j R_{j\to i}x_j = 0 \\ -1 & \text{if } \sum_j R_{j\to i}x_j < 0, \end{cases} \quad \forall i.$$

To generate random networks, we need to randomly fill in 1 or -1 for the regulatory matrix $\mathbf{R} = (R_{j\to i})$. For this first ensemble, we follow the generation procedure in [39] to randomly add edges between pairs of genes and form a combined structural and functional ensemble (**Ensemble-1**) based on the budding yeast cell cycle network (shown in Fig. 4), which has 11 genes ($n = 11$). Each of these randomly generated networks has the same number of nodes, the same number of activating edges, and the same number of suppressing edges as the original cell cycle network (i.e., 11 nodes, 15 activating regulations, 19 suppressing regulations). Moreover, they all produce the same state transition trajectory subsequence, which is essential to the corresponding cell cycle process [35], [39]: in the order of genes Cln3, MBF, SBF, Cln1,2, Clb5,6, Clb1,2, Mcm1, Cdc20, Swi5, Sic1, and Cdh1, the network state transitions from the "excited" G1 phase (10000000011 → 01100000011 → 01110000011 →01110000000), going through the S state (01111000000), the G2 state (01111110000), then to the M phase (00011111000 → 000001111000 → 000001111100 →00000001111), and finally returning to the biological G1 stationary state (00000000011).

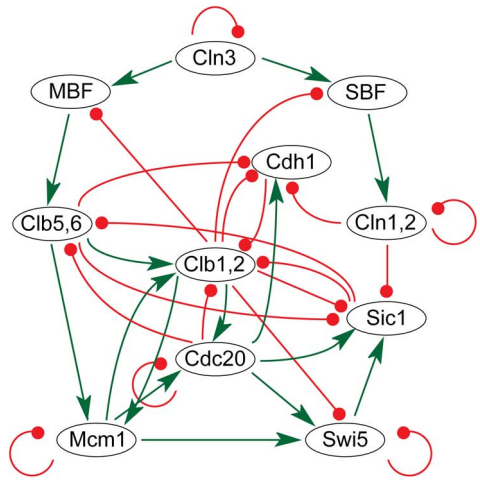

Fig. 4. *Saccharomyces cerevisiae* cell cycle network modified from [35]: the green arrows represent activation and the red arrows with solid circles represent suppression.

TABLE III
THE AVERAGE NUMBER m_d OF RANDOM NETWORKS WITH DIFFERENT ψ^* FROM ANY MODEL SPECIFIC STRUCTURAL INTERVENTION ψ_θ AND ITS STANDARD DEVIATION σ_d IN TWO RANDOM ENSEMBLES

	Ensemble	**1**	**Ensemble**	**2**
D	m_d	σ_d	m_d	σ_d
1	0.9000	0.8756	0.2000	0.0020
2	1.8000	0.7888	0.0000	0.0000
3	2.1000	0.9944	0.0000	0.0000
4	2.2000	2.0440	0.0000	0.0000

In the second approach, we create the random ensembles (**Ensemble-2**) by generating random networks with the same number of nodes ($n = 11$), but instead of forming a structural and functional ensemble based on a given biological network as in **Ensemble-1**, we randomly fill the regulatory matrix $\mathbf{R}$ by first determining the number of regulators K_i for each gene i and then randomly picking 1 or -1 for $R_{j\to i}$ with j as one of the K_i regulators for gene i. In our simulations, we pick the K_i regulators among the $n = 11$ genes with the uniform probability, $\forall i$. As studied in [52], the random BNps in the first ensemble possess relatively more stable network dynamics, which means that the regulatory relationships of random networks in this combined structural and functional ensemble are mostly critical for generating the previously specified state transitions. On the other hand, in the second ensemble, we do not put any restrictions on regulation configuration or state transitions. As a result, the probability of a randomly selected regulation $R_{j\to i}$ being critical for network dynamics will be lower than that in the first random ensemble. For this reason, we expect that the chance that the optimal robust intervention ψ^* (i.e., IBR operator) would be different from the MCBR structural intervention $\psi_{\hat{\varphi}}$ will be larger for **Ensemble-1** than the chance for **Ensemble-2**.

To confirm our conjecture, we generated 100 random networks in each ensemble and further randomly picked 10 independent sets of regulations and assumed their activating/suppressing relationships to be uncertain, each set containing $1 \le D \le 4$ uncertain regulations. For all these random networks, we set the perturbation probability to $p = 0.01$. In Table III,

we show the average number m_d (and the standard deviation σ_d) of random networks with uncertainty for which the IBR intervention was different from the MCBR intervention (i.e., $\psi^* \neq \psi_{\hat{\varphi}}$). As expected, we can see that the combined structural and functional ensemble (**Ensemble-1**) has a larger m_d. More interestingly, the average number m_d for **Ensemble-1** increases gradually with the number of uncertain regulations D. This is reasonable, since the optimal robust strategy ψ^* will be more likely to be different from any network-specific intervention ψ_θ as the model uncertainty increases with increasing D. However, in **Ensemble-2**, m_d is non-zero only when $D = 1$, which clearly shows that the randomly selected regulations in this ensemble may not be very critical from the perspective of network dynamics. In this case, with increasing D, the probability of selecting a set of uncertain regulations that include critical regulations decreases, since the number of simulations in our experiments is relatively small compared to the size of the uncertainty class, which increases exponentially with D; and thereafter we observe $m_d = 0$ when $D > 1$. In fact, the trend of m_d is complicated, which makes further theoretical analysis very difficult. Generally, m_d will depend on the properties of the considered networks as well as the nature of the uncertainty in those networks that give rise to the uncertainty class Θ. However, the present simulations clearly demonstrate that objective-based UQ framework and the concept of MOCU can effectively capture the critical properties and dynamics of gene regulatory networks that are pertinent to our goal (i.e., structural intervention in this example), in the presence of substantial uncertainty.

D. Robust Structural Intervention in the Mammalian Cell Cycle Network

Next, we consider the application of the proposed objective-based UQ framework to the robust structural intervention in a mammalian cell cycle network [34]. As before, we set the perturbation probability to $p = 0.01$ and adopt the logic Boolean transition functions based on the "majority vote" rules. The considered mammalian cell cycle network consists of $n = 10$ genes (CycD, Rb, p27, E2F, CycE, CycA, Cdc20, Cdh1, UbcH10, and CycB), whose regulatory relationships are depicted in Fig. 5. For normal mammalian organisms, cell division is controlled via extra-cellular signals and it is coordinated with overall growth. The positive signals, or growth factors, instigate CycD. The cyclins inhibit Rb by phosphorylation and hence Rb is expressed in the absence of cyclins. The gene p27 can stop the uncontrolled cell cycle as it blocks the action of CycE or CycA and thereafter Rb can also be expressed, even in the presence of CycE or CycA. We model this by a BNp with x_i denoting each of the ten genes in the same order as we previously introduced them. In this model, the network states where CycD, Rb, and p27 are simultaneously down-regulated (i.e., $x_1 = x_2 = x_3 = 0$) represent cancerous phenotypes, in which the cell cycles even in the absence of any growth factor. Therefore, we define these network states as undesirable states $U = \{\mathbf{x} | x_1 = x_2 = x_3 = 0\}$.

Fig. 6 shows the steady-state distribution of the given network, where the undesirable probability mass is $\pi_U = \sum_{x_1=0,x_2=0,x_3=0} \pi_{\mathbf{x}} = 0.3401$. In order to investigate the trends of the MOCU $\mathrm{M}_{\Psi,\Xi,f}(\Theta)$ (based on IBR intervention) and approximate model-constrained MOCU $\mathrm{M}^{\mathrm{mc}}_{\Psi,\Xi,f}(\Theta)$ (based on MCBR intervention) for varying amounts of uncertainty, we assumed that the regulatory information $R_{j\to i}$ (activating or suppressing) is unknown for a set of edges in the network. The class of structural intervention strategies Φ is comprised of perturbations that block the regulatory action between any pair of genes in the network (by setting $R_{j\to i} = 0$). Given the full knowledge of the network (without any unknown regulatory relationship), we can derive the optimal structural intervention, which is to block the regulatory action from gene CycE to p27 (marked in red in Fig. 5). That minimizes the undesirable mass to $\tilde{\pi}_U^{opt} = 0.2639$.

Based on the given network, we ran simulations to derive the IBR and MCBR structural intervention strategies and to compute the resulting MOCU for several different network classes, obtained by incrementally increasing the number of

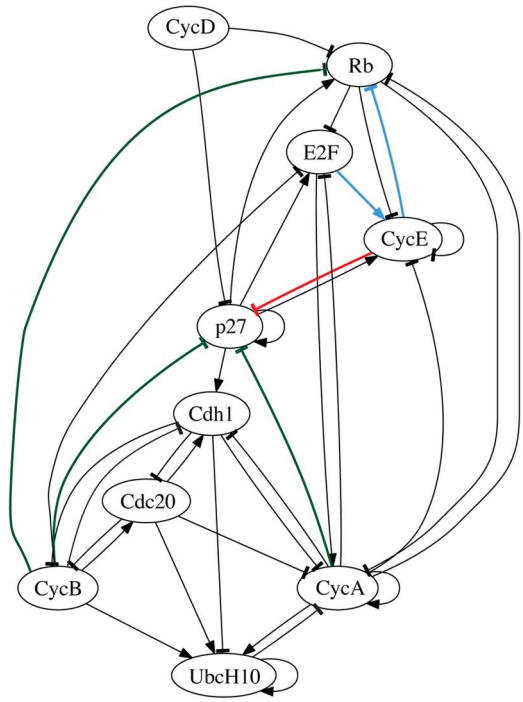

Fig. 5. Mammalian cell cycle network modified from [34]: Normal arrows represent activations and blunt arrows represent suppressing effects. Given the full knowledge of the network, the optimal intervention strategy is to block the regulation from CycE to p27 (shown in red). Other regulations to be blocked according to the IBR intervention strategies, in the absence of full regulatory information, are shown in bright blue and dark green. The two IBR strategies blocking the edges marked in bright blue lead to significant reduction of undesirable steady-state mass that is comparable to the optimal strategy.

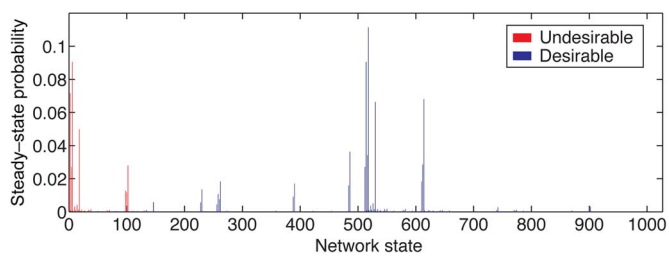

Fig. 6. The steady-state distribution of the BNp that models the mammalian cell cycle network.

TABLE IV
THE SELECTION FREQUENCY OF THE IBR AND MCBR INTERVENTION STRATEGIES FOR 50 RANDOM UNCERTAIN NETWORKS. NOTE THAT THERE ARE ONLY NINE DERIVED IBR STRATEGIES FOR THESE RANDOM CASES WHILE THERE ARE TEN MCBR STRATEGIES

Intervention	IBR(1 : 5)	MCBR(1 : 5)	IBR(1 : 10)	MCBR(1 : 10)	$\tilde{\pi}_U$
(CycE,p27)	54.0%	55.2%	50.0%	51.0%	0.2639
(CycE,Rb)	41.6%	39.6%	38.6%	37.8%	0.2643
(CycB,p27)	2.0%	0.8%	4.0%	3.4%	0.3244
(CycA,p27)	1.2%	1.2%	1.8%	1.8%	0.3189
(E2F,CycE)	0.8%	0.8%	0.6%	0.6%	0.2683
(CycB,Rb)	0.4%	0.4%	1.6%	1.2%	0.3314
(Rb,CycE)	−−	0.8%	0.4%	0.8%	0.3842
(CycD,p27)	−−	−−	1.6%	1.4%	0.3205
(CycA,Rb)	−−	−−	1.4%	1.4%	0.3294
(Cdh1,CycB)	−−	1.2%	−−	0.6%	0.3404

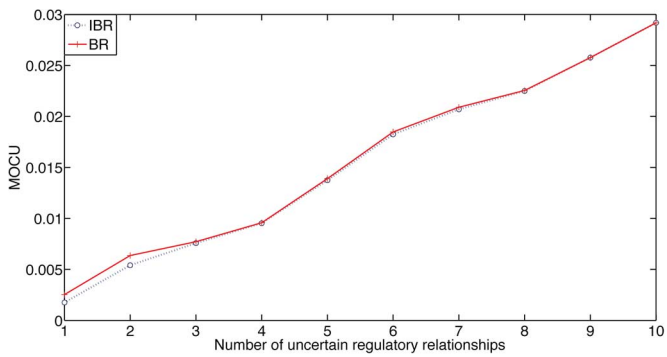

Fig. 7. MOCU $\mathrm{M}_{\Psi,\Xi,f}(\Theta)$ (based on IBR intervention) and model-constrained MOCU $\mathrm{M}^{\mathrm{mc}}_{\Psi,\Xi,f}(\Theta)$ (based on MCBR intervention) for different number of uncertain edges in the mammalian cell cycle network.

edges with unknown regulation from $D = 1$ to $D = 10$. In each case, we sampled 50 networks by randomly selecting D uncertain edges, while keeping the regulatory information for the remaining edges. Fig. 7 shows the estimated MOCU $\mathrm{M}_{\Psi,\Xi,f}(\Theta)$ and the model-constrained MOCU $\mathrm{M}^{\mathrm{mc}}_{\Psi,\Xi,f}(\Theta)$ for an increasing number of uncertain edges D. Intuitively, as D increases (i.e., larger number of uncertain edges), the cost of uncertainty—or the performance degradation of the robust intervention strategy measured in terms of its capability to shift the undesirable steady-state mass—would also increase. The simulation results confirm this intuition, as shown by the increase of $\mathrm{M}_{\Psi,\Xi,f}(\Theta)$ and $\mathrm{M}^{\mathrm{mc}}_{\Psi,\Xi,f}(\Theta)$ for increasing number of uncertain regulatory relationships in the network. Fig. 7 also shows that the model-constrained MOCU $\mathrm{M}^{\mathrm{mc}}_{\Psi,\Xi,f}(\Theta)$ serves as an upper-bound of the true MOCU $\mathrm{M}_{\Psi,\Xi,f}(\Theta)$. Furthermore, the figure shows that the discrepancy between $\mathrm{M}_{\Psi,\Xi,f}(\Theta)$ and $\mathrm{M}^{\mathrm{mc}}_{\Psi,\Xi,f}(\Theta)$ is relatively small for this example, which implies that the model-constrained MOCU may serve as a good index for characterizing the objective-based cost of uncertainty, when the computational cost for computing the true MOCU is prohibitively high.

We further investigated the IBR and MCBR robust structural intervention strategies that were derived for the mammalian cell cycle network in the presence of uncertain edges. Table IV lists the derived IBR and MCBR intervention strategies with their selection frequency among 50 networks with different number of random uncertain edges. (A, B) denotes the regulation from A to B that needs to be blocked according to a given intervention strategy. We show the selection frequency for random networks with $1 \sim 5$ uncertain edges (denoted as 1:5 in the table) as well as the frequency for networks with $1 \sim 10$ uncertain edges (denoted as 1:10). The rightmost column in Table IV shows the steady-state probability mass in undesirable states after applying a given intervention strategy to the original mammalian cell cycle network.

For networks that contain no more than five uncertain edges, a total of six different IBR strategies have been derived, which included the optimal intervention strategy for the original network. All six IBR strategies indeed lead to beneficial structural intervention which reduces the undesirable steady-state mass. These six robust strategies include the top three intervention strategies that lead to the smallest undesirable steady-state mass: (i) the actual optimal strategy, which is to block the regulation from CycE to p27, (ii) a different strategy, which is to block the regulation from CycE to Rb, and (iii) another strategy, in which we block the regulation from E2F to CycE. These three intervention strategies lead to comparable results, where the undesirable steady-state masses (relative to the true network) are $\tilde{\pi}_U = 0.2639$, $\tilde{\pi}_U = 0.2643$, and $\tilde{\pi}_U = 0.2683$, respectively. In Fig. 5, the optimal strategy is shown in red and the other two effective strategies are shown in bright blue. The remaining three IBR intervention strategies (shown in dark green) were also beneficial, although not as effective as the aforementioned strategies. Among these three strategies, blocking the regulation from CycA to p27 leads to a reduced undesirable steady-state mass of $\tilde{\pi}_U = 0.3189$; blocking the regulation from CycB to p27 yields $\tilde{\pi}_U = 0.3244$; and blocking the regulation from CycB to Rb results in $\tilde{\pi}_U = 0.3314$. For networks with up to five uncertain edges, the derived MCBR strategies included two additional intervention strategies that were not among the six IBR strategies. These two MCBR intervention strategies are to block the regulation from Cdh1 to CycB, and the one from Rb to CycE, both of which in fact increase the undesirable steady-state probability mass to $\tilde{\pi}_U = 0.3404$ and 0.3842, respectively. This example shows that the MCBR strategy may result in a lower performance compared to the IBR strategy, as it is constrained to network-specific strategies for networks that belong to the uncertainty class at hand.

For networks with more than five uncertain edges, we obtained two additional robust strategies, which are also shown

in Table IV. Among all these robust strategies, eight of them are beneficial and only two lead to increased undesirable steady-state mass. As shown in this table, the intervention performance may degrade when the uncertainty increases. We can also observe in Table IV that for more than 88% of the considered networks (with random uncertain regulations), both IBR and MCBR methods predicted the top two intervention strategies—blocking the regulation from CycE to p27 (optimal) or the regulation from CycE to Rb—that result in substantial decrease of undesirable steady-state mass, clearly demonstrating the potential of the proposed objective-based UQ framework for deriving effective intervention strategies in the presence of significant network uncertainty.

Finally, it is worth noting that the beneficial robust structural intervention strategies target at regulatory relationships that connect important genes in the cell cycle network—including the cyclins (CycA, CycB, CycE), E2F, Rb, and p27—that have been reported to play critical roles in the ability of a cell to reverse the R(estriction)-point. This marks a critical event when a mammalian cell commits to proliferation independent of growth stimulation, corresponding to cancerous situations [53]. This demonstrates that the robust structural intervention strategies, derived based on the proposed UQ framework, can accurately identify and effectively target the optimal network control points that are critical in beneficially altering the network dynamics to achieve the ultimate objective.

V. Concluding Remarks

In this paper, we proposed a novel objective-based uncertainty quantification (UQ) framework that can be effectively used for quantifying and handling uncertainty in complex systems. The proposed scheme quantifies the uncertainty in terms of the expected increase of the operational cost—referred to as MOCU (mean objective cost of uncertainty)—that is induced by our imperfect knowledge of the system of interest. We applied the proposed UQ framework for quantifying the uncertainty in gene regulatory networks with unknown regulations, modeled using PBNs. As demonstrated in our simulation results, MOCU can accurately capture the amount of uncertainty in a given network and guide us to design robust operators (i.e., robust structural intervention strategies in this case) that would result in the optimal expected performance, or minimal operational cost, in the presence of substantial uncertainty.

The practical import of having a means of quantifying the cost of uncertainty relative to a given objective—such as the MOCU proposed in this paper—is that it can provide an operational theory with a natural framework within which the operational effect of uncertainty can be quantified. Not only would the existence of such a framework provide a deeper understanding of the practical nature of the uncertainty, it would also facilitate model analysis and development in several important areas such as complexity analysis, objective-based model reduction, and experimental design for optimal reduction of model uncertainty. Although we have focused on the structural intervention of PBNs in this paper, it should be noted that the proposed UQ-framework is fairly general and it can be applied to other models and applications, when there is a need for quantifying and handling uncertainty.

References

[1] I. Shmulevich and E. R. Dougherty, *Genomic Signal Processing*. Princeton, NJ, USA: Princeton Univ. Press Princeton, 2007.

[2] V. Kuznetsov, "Stable detection when the signal and spectrum of normal noise are inaccurately known," *Telecommun. Radio Eng.*, vol. 30, p. 31, 1976.

[3] S. Kassam and T. Lim, "Robust Wiener filters," *J. Franklin Inst.*, vol. 304, no. 4–5, pp. 171–185, 1977.

[4] H. Poor, "On robust Wiener filtering," *IEEE Trans. Autom. Control* , vol. 25, no. 3, pp. 531–536, 1980.

[5] K. Vastola and H. Poor, "Robust Wiener-Kolmogorov theory," *IEEE Trans. Inf. Theory*, vol. 30, no. 2, pp. 316–327, 1984.

[6] S. Verdu and H. Poor, "Minimax linear observers and regulators for stochastic systems with uncertain second-order statistics," *IEEE Trans. Autom. Control*, vol. 29, no. 6, pp. 499–511, 1984.

[7] E. Dougherty and Y. Chen, "Robust optimal granulometric bandpass filters," *Signal Process.*, vol. 81, no. 7, pp. 1357–1372, 2001.

[8] E. Dougherty, J. Hua, Z. Xiong, and Y. Chen, "Optimal robust classifiers," *Pattern Recogn.*, vol. 38, no. 10, pp. 1520–1532, 2005.

[9] R. Pal, A. Datta, and E. Dougherty, "Bayesian robustness in the control of gene regulatory networks," *IEEE Trans. Signal Process.*, vol. 57, no. 9, pp. 3667–3678, 2009.

[10] T. Ideker, V. Thorsson, and R. Karp, "Discovery of regulatory interactions through perturbation: Inference and experimental design," in *Proc. Pacific Symp. Biocomput.*, 2000, vol. 5, pp. 302–313.

[11] A. Almudevar and P. Salzman, "Using a Bayesian posterior density in the design of perturbation experiments for network reconstruction," in *Proc.. IEEE Symp. Computat. Intell. Bioinform. Computat. Biol. (CIBCB'05)*, 2005, pp. 1–7.

[12] E. Lehmann and G. Casella, *Theory of Point Estimation*. New York, NY, USA: Springer, 1998, vol. 31.

[13] D. Berry and B. Fristedt, *Bandit Problems: Sequential Allocation of Experiments*. London, U.K.: Chapman & Hall, 1985.

[14] J. Bernardo and A. Smith, "Bayesian theory," *Measure. Sci. Technol.*, vol. 12, no. 2, p. 221, 2001.

[15] M. Clyde and E. George, "Model uncertainty," *Statist. Sci.*, pp. 81–94, 2004.

[16] D. Madigan and A. Raftery, "Model selection and accounting for model uncertainty in graphical models using Occam's window," *J. Amer. Statist. Assoc.*, vol. 89, no. 428, pp. 1535–1546, 1994.

[17] M. Barbieri and J. Berger, "Optimal predictive model selection," *Ann. Statist.*, vol. 32, no. 3, pp. 870–897, 2004.

[18] M. Chen, J. Ibrahim, Q. Shao, and R. Weiss, "Prior elicitation for model selection and estimation in generalized linear mixed models," *J. Statist. Plann. Infer.*, vol. 111, no. 1, pp. 57–76, 2003.

[19] H. Chipman, E. George, R. McCulloch, M. Clyde, D. Foster, and R. Stine, "The practical implementation of Bayesian model selection," *Lecture Notes-Monograph Ser.*, pp. 65–134, 2001.

[20] J. Hoeting, D. Madigan, A. Raftery, and C. Volinsky, "Bayesian model averaging: A tutorial," *Statist. Sci.*, pp. 382–401, 1999.

[21] A. Raftery, D. Madigan, and J. Hoeting, "Bayesian model averaging for linear regression models," *J. Amer. Statist. Assoc.*, vol. 92, no. 437, pp. 179–191, 1997.

[22] A. Merlise, "Bayesian model averaging and model search strategies," in *Proc. 6th Valencia Int. Mtg. Bayesian Statist.*, 1999, vol. 6, p. 157, Oxford Univ. Press.

[23] L. Wasserman, "Bayesian model selection and model averaging," *J. Mathemat. Psychol.*, vol. 44, no. 1, pp. 92–107, 2000.

[24] C. Andrieu, A. Doucet, and C. Robert, "Computational advances for and from Bayesian analysis," *Statist. Sci.*, vol. 19, no. 1, pp. 118–127, 2004.

[25] L. R. Rabiner, "A tutorial on hidden Markov models and selected applications in speech recognition," *Proc. IEEE*, vol. 77, no. 2, pp. 257–286, 1989.

[26] Y. Chen and B. Chen, "Minimax robust deconvolution filters under stochastic parametric and noise uncertainties," *IEEE Trans. Signal Process.*, vol. 42, no. 1, pp. 32–45, 1994.

[27] C. Chen and S. Kassam, "Robust multiple-input matched filtering: Frequency and time-domain results," *IEEE Trans. Inf. Theory*, vol. 31, no. 6, pp. 812–821, 1985.

[28] H. Poor, "Robust matched filters," *IEEE Trans. Inf. Theory*, vol. 29, no. 5, pp. 677–687, 1983.

[29] V. Poor and D. Looze, "Minimax state estimation for linear stochastic systems with noise uncertainty," *IEEE Trans. Autom. Control*, vol. 26, no. 4, pp. 902–906, 1981.

[30] W. Zheng, A. Cantoni, and K. Teo, "Robust design of envelope-constrained filters in the presence of input uncertainty," *IEEE Trans. Signal Process.*, vol. 44, no. 8, pp. 1872–1878, 1996.

[31] A. Grygorian and E. Dougherty, "Bayesian robust optimal linear filters," *Signal Process.*, vol. 81, no. 12, pp. 2503–2521, 2001.
[32] I. Shmulevich, E. Dougherty, S. Kim, and W. Zhang, "Probabilistic Boolean networks: A rule-based uncertainty model for gene regulatory networks," *Bioinformat.*, vol. 18, no. 2, pp. 261–274, 2002.
[33] S. Kauffman, "Metabolic stability and epigenesis in randomly constructed genetic nets," *J. Theoret. Biol.*, vol. 22, pp. 437–467, 1969.
[34] A. Faure, A. Naldi, C. Chaouiya, and D. Theiffry, "Dynamical analysis of a generic boolean model for the control of the mammalian cell cycle," *Bioinformat.*, vol. 22, no. 14, pp. 124–131, 2006.
[35] F. Li, T. Long, Y. Lu, Q. Ouyang, and C. Tang, "The yeast cell-cycle network is robustly designed," *Proc. Nat. Acad. Sci. USA*, vol. 101, no. 14, pp. 4781–4786, 2004.
[36] M. Davidich and S. Bornholdt, "Boolean network model predicts cell cycle sequence of fission yeast," *PLoS ONE*, vol. 3, no. e1672, 2008.
[37] Y. Wu, X. Zhang, J. Yu, and Q. Ouyang, "Identification of a topological characteristic responsible for the biological robustness of regulatory networks," *PLoS Computat. Biol.*, vol. 5, no. 7, 2009.
[38] X. Qian and E. Dougherty, "Effect of function perturbation on the steady state distribution of genetic regulatory networks: Optimal structural intervention," *IEEE Trans. Signal Process.*, vol. 56, no. 10, pp. 4966–4976, 2008.
[39] K. Lau, S. Ganguli, and C. Tang, "Function constrains network architecture and dynamics: A case study on the yeast cell cycle Boolean network," *Phys. Rev. E*, vol. 75, p. 051907, 2007.
[40] A. Garg, A. Di Cara, I. Xenarios, L. Mendoza, and G. De Micheli, "Synchronous versus asynchronous modeling of gene regulatory networks," *Bioinform.*, vol. 24, pp. 1917–1925, 2008.
[41] B. Faryabi, J. Chamberland, G. Vahedi, A. Datta, and E. Dougherty, "Optimal intervention in asynchronous genetic regulatory networks," *IEEE J. Sel. Top. Signal Process.*, vol. 2, no. 3, pp. 412–423, 2008.
[42] J. Kemeny and J. Snell, *Finite Markov Chains*. New York, NY, USA: Van Nostrand, 1960.
[43] P. Schweitzer, "Perturbation theory and finite Markov chains," *J. Appl. Probab.*, vol. 5, pp. 401–413, 1968.
[44] A. Datta, R. Pal, A. Choudhary, and E. Dougherty, "Control approaches for probabilistic gene regulatory networks," *IEEE Signal Process. Mag.* , vol. 24, no. 1, pp. 54–63, 2007.
[45] I. Shmulevich and E. R. Dougherty, *Probabilistic Boolean Networks: The Modeling and Control of Gene Regulatory Networks*. Philadelphia, PA, USA: SIAM, 2010.
[46] R. Pal, A. Datta, and E. Dougherty, "Optimal infinite-horizon control for probabilistic Boolean networks," *IEEE Trans. Signal Process.*, vol. 54, no. 6, pp. 2375–2387, 2006.
[47] M. Cusick, H. Yu, and A. Smolyar *et al.*, "Literature-curated protein interaction datasets," *Nat. Methods*, vol. 6, pp. 39–46, 2009.
[48] M. Newman, A.-L. Barabasi, and D. Watts, *The Structure and Dynamics of Networks*. Princeton, NJ, USA: Princeton Univ. Press, 2006.
[49] N. Perra and S. Fortunato, "Spectral centrality measures in complex networks," *Phys. Rev. E Stat Nonlin. Soft Matter Phys.*, vol. 78, no. 3 Pt. 2, p. 036107, 2008.
[50] A. Potapov, B. B. Goemann, and E. Wingender, "The pairwise disconnectivity index as a new metric for the topological analysis of regulatory networks," *BMC Bioinform.*, vol. 9, p. 227, 2008.
[51] Y. Liu, J.-J. Slotine, and A.-L. Barabasi, "Controllability of complex networks," *Nature*, vol. 473, pp. 167–173, 2011.
[52] X. Qian and E. Dougherty, "A comparative study on sensitivities of Boolean networks," in *Proc. IEEE Int. Workshop on Genom. Signal Process. Statist. (GENSIPS)*, Nov. 2010, pp. 1–4.
[53] G. Yao, T. Lee, S. Mori, J. Nevins, and L. You, "A bistable myc-rb-e2f switch: A model for the restriction point," *Nat. Cell Biol.*, vol. 10, pp. 476–482, 2008.

Byung-Jun Yoon (S'01–M'07–SM'11) received the B.S.E. (*summa cum laude*) degree from Seoul National University (SNU), Seoul, Korea, in 1998, and the M.S. and Ph.D. degrees from California Institute of Technology (Caltech), Pasadena, in 2002 and 2007, respectively, all in electrical engineering.

In 2008, he joined the Department of Electrical and Computer Engineering, Texas A&M University, College Station, where he is currently an Assistant Professor. His main research interests include genomic signal processing, bioinformatics, and computational biology.

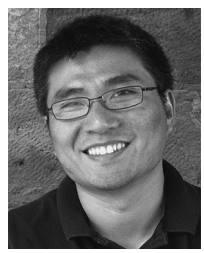

Xiaoning Qian (S'01–M'07) received the Ph.D. degree in electrical engineering from Yale University, New Haven, CT, in 2005.

Currently, he is an Assistant Professor with the Department of Computer Science and Engineering, University of South Florida, Tampa. He was with the Bioinformatics Training Program, Texas A&M University, College Station. His current research interests include computational biology, genomic signal processing, and biomedical image analysis.

Edward R. Dougherty (M'05–SM'09–F'11) received the Ph.D. degree in mathematics from Rutgers University, New Brunswick, NJ, and the M.S. degree in computer science from Stevens Institute of Technology, Hoboken, NJ, and has been awarded the Doctor Honoris Causa by the Tampere University of Technology, Finland.

He is a Professor with the Department of Electrical and Computer Engineering, Texas A&M University, College Station, where he holds the Robert M. Kennedy 26 Chair in Electrical Engineering and is Director of the Genomic Signal Processing (GSP) Laboratory. He is also Co-Director of the Computational Biology Division of the Translational Genomics Research Institute (TGen), Phoenix, AZ.

Dr. Dougherty is a Fellow of SPIE. He has received the SPIE Presidents Award, and served as the Editor of the SPIE/IS&T *Journal of Electronic Imaging*.